POLITECNICO
MILANO 1863

SCUOLA DI INGEGNERIA INDUSTRIALE
E DELL'INFORMAZIONE

Executive Summary of the Thesis

High-speed ultrabroadband CARS microscopy based on supercontinuum generation in bulk media

Laurea Magistrale in Engineering Physics - Ingegneria Fisica

Author: Francesco Gucci

Advisor: Prof. Dario Polli

Co-advisor: Federico Vernuccio

Academic year: 2021-2022

1. Introduction

Every biological sample has a vibrational spectrum representing its molecular structure and offering an endogenous unique signature that can be used for the identification of its chemical constituents. Spontaneous Raman (SR) microscopy is a powerful label-free optical tool to measure vibrational spectra. It exploits quasi-monochromatic laser light at frequency ω_P (pump frequency) in the visible or near-infrared to excite a molecule to a virtual state, from which it relaxes to the ground state emitting a photon with lower energy at frequency ω_S (Stokes frequency). The Stokes frequency, $\omega_S = \omega_p - \Omega$, is red shifted in frequency and carries the vibrational information at frequency Ω. The resulting spectrum consists in a superposition of peaks, each representing a specific chemical bond, and could be divided into three main regions: the fingerprint region (400-1800 cm^{-1}), which has a high number of peaks and is considered to be the most informative one for biological samples since many contributions from proteins and nucleic acids can be observed in this interval, the silent region (1800-2800 cm^{-1}), which has no peaks, and the carbon-hydrogen (C-H) stretching region (2800-3100 cm^{-1}). SR suffers from several limitations, mainly due to the low scattering cross section, which implies weak signal and long integration times, preventing the achievement of high acquisition speeds, and due to the incoherence of the process, released isotropically from the material. Coherent Raman Scattering (CRS) overcomes these limitations exploiting third-order nonlinear optical processes which allow generating a signal higher than the SR one up to a factor of 10^7 [1]. CRS exploits the simultaneous interaction of two ultrashort light pulses, pump (at ω_P) and a red-shifted Stokes (at ω_S), with a medium. When the difference between the two frequencies, $\Omega = \omega_P - \omega_S$, matches a vibrational frequency of the sample, a collective molecular oscillation is induced in the focal volume emitting a coherent and stronger signal. Among the CRS processes, coherent anti-Stokes Raman scattering (CARS) is analyzed and experimentally exploited in this work. In the CARS process, the vibrational coherence is generated by an encounter with a probe beam at frequency ω_{PR}, producing coherent radiation at the anti-Stokes frequency $\omega_{AS} = \omega_{PR} + \Omega$ (usually, $\omega_{PR} = \omega_P$ is used so that $\omega_{AS} = \omega_P + \Omega$). Since the CARS signal arises in a region of the spectrum blue-

shifted with respect to the pump and Stokes beams, it can be easily detected using a spectrometer, after a filter that removes the generating beams. However, CARS features distorted spectral lineshapes due to the presence of a non resonant background (NRB) deriving from four-wave mixing processes concurrently occurring at the sample plane with the resonant ones. These distortions prevent a direct comparison of the CARS signal with the SR one.
Extremely high acquisition speeds detecting the CARS signal have already been demonstrated in the single-frequency regime, where pump and Stokes are narrowband picosecond pulses allowing one to probe only a specific vibrational mode. This approach does not allow one to distinguish different biochemical species which tipically are spatially superimposed in heterogeneous samples. Hence, it calls for Broadband CARS (B-CARS) microscopy, where full spectra may be acquired in a single shot [2]. A possible implementation of B-CARS is multiplex B-CARS, that combines a broadband Stokes pulse and a narrowband pump pulse to illuminate the sample. SC generation is usually achieved in tapered fiber or photonic crystal fiber [3]. In this work, an innovative experimental configuration for multiplex ultra-broadband CARS with SC generation in bulk media is described and the experimental results are shown. SC in bulk media represents a more compact, reliable, easy-to-use, and alignment-insensitive approach [4]. When a high-intensity pulse propagates in a transparent medium, many optical non-linear processes are stimulated simultaneously, giving rise to a complex coupling between spatial and temporal effects. In particular, the interplay between self focusing, due to optical Kerr effect, and defocusing, due to propagation in induced free electron plasma, gives rise to optical filamentation. During the propagation in the optical filament, the pulse keeps a narrow beam size and its spectrum is broadened by Self Phase modulation and chromatic dispersion. The detection of the B-CARS signal is performed in the frequency domain, simply using a spectrometer dispersing the anti-Stokes components and a CCD. This approach reaches lower than 1 ms pixel dwell time, which is the limit of commercial CCD sensors.

2. Theory

In this section, the basic theory regarding the studied processes is presented. When the peak intensity of a pulse overcomes a certain threshold, namely $I_{peak} > 10^{8-9}\frac{W}{cm^2}$, the matter response becomes non-linear and can be described through a perturbative approach. In this case, the polarization has two main components: $P = P^{(L)} + P^{(NL)}$, where $P^{(L)}$ represents the linear polarization, while $P^{(NL)}$ is the non-linear one, and can be further developed as the sum of many components with different order of non-linearity, as reported in (1):

$$P^{(NL)} = \sum_{n=2}^{\infty} P^{(n)} = P^{(2)} + P^{(3)} + \dots. \quad (1)$$

Since the CARS signal arises from a third order interaction, we will focus on such phenomena. The third order polarization reads as:

$$P^{(3)} = \epsilon_0 \chi^{(3)} E^3(t), \quad (2)$$

Where $\chi^{(3)}$ is the third order susceptibility. The electric field is characterised by the presence of a pump and a Stokes pulses, and is defined as:

$$E(z,t) = \frac{1}{2}\{A_P e^{i(\omega_P t - k_P z)} + \\ + A_S e^{i(\omega_S t - k_S z)} + c.c.\}, \quad (3)$$

Where A_i are the envelope of the propagating pulses, ω_i are the central frequencies and k_i are the wavenumbers. The interference between the two fields generates a beating with frequency $\Omega = \omega_P - \omega_S$, in which P and S stand for pump and Stokes. If the beating frequency Ω matches the frequency of a vibrational mode, $\Omega_R = \Omega$, then the normal mode enters in resonance with the wave beating. We can now plug (3) in (2), and write the polarization as:

$$P_{\omega_{AS}} = f A_P^2 A_S^* e^{i[\omega_{AS} t - (2k_P - k_S)z]} + c.c., \quad (4)$$

Where $f = \frac{3\epsilon_0 \chi^{(3)}(\omega_{AS})}{4}$. The polarization reported in (4) gives rise to the CARS signal at frequency $\omega_{AS} = 2\omega_P - \omega_S$, with intensity:

$$I_{AS}(L) \propto |\chi^{(3)}|^2 L^2 \,\mathrm{sinc}^2\left(\frac{\Delta k L}{2}\right) I_P^2 I_S, \quad (5)$$

Where $\Delta k = 2k_P - k_S - k_{AS}$. We can observe that the CARS signal depends quadratically on

the pump intensity and linearly on the Stokes one. In order to get high intensity, the phase matching condition should be respected, namely $\Delta k = 2k_P - k_S - k_{AS} \simeq 0$, however, in condition of tight focusing, which can be assumed in microscopy, ΔkL is approximately equal to zero, therefore, eq. (5) can be simplified obtaining: $I_{AS}(L) \propto |\chi^{(3)}|^2 L^2 I_P^2 I_S$. The CARS intensity depends on $|\chi^{(3)}|^2$, where $\chi^{(3)}$ can be written as the sum of a resonant and a non-resonant parts: $\chi^{(3)} = \chi_R^{(3)} + \chi_{NR}^{(3)}$. The resonant part $\chi_R^{(3)}$ depends on the beating frequency Ω , it is characterized by a real and an imaginary parts and it is related to the vibrational modes by the expression:

$$\chi_R^{(3)}(\Omega) = \sum_{i=1}^{M} \frac{a_i}{(\Omega - \Omega_{R_i}) + i\gamma_i} \qquad (6)$$

Where a_i is a number representing the oscillator strength of the i-th molecular mode of vibration, Ω_{R_i} is the resonance frequency of the i-th mode and γ_i is a damping term. When Ω matches one of the resonance frequencies, $\chi_R^{(3)}$ is enhanced. The non-resonant part $\chi_{NR}^{(3)}$ originates from the instantaneous electronic response of the medium and is real and constant if far from electronic resonances. We can now develop the CARS intensity dependence on $\chi^{(3)}$:

$$I_{AS} \propto \left|\chi_R^{(3)}\right|^2 + \left|\chi_{NR}^{(3)}\right|^2 + 2\chi_{NR}^{(3)} Re\left[\chi_R^{(3)}\right], \quad (7)$$

Analyzing eq. (7), it is possible to observe that the CARS intensity is the sum of three different contributions:

1. A resonant contribution, given by the term $\left|\chi_R^{(3)}\right|^2$. This term contains the information regarding the vibrational modes and it is meaningful in spectroscopy applications.
2. A non-resonant contribution, given by the term $\left|\chi_{NR}^{(3)}\right|^2$. This term is almost constant in the spectral domain if far from electronic resonances.
3. In the last term, $2\chi_{NR}^{(3)} Re\left[\chi_R^{(3)}\right]$, the resonant and non-resonant parts are mixed together giving rise to a heterodyne contribution.

The CARS spectrum appears distorted with respect to the SR spectrum due to the contributions of the second and third terms of the equation, which give rise to the so called Non-resonant Background (NRB). A representation of the different contributions to the CARS signal is reported in fig. 1.

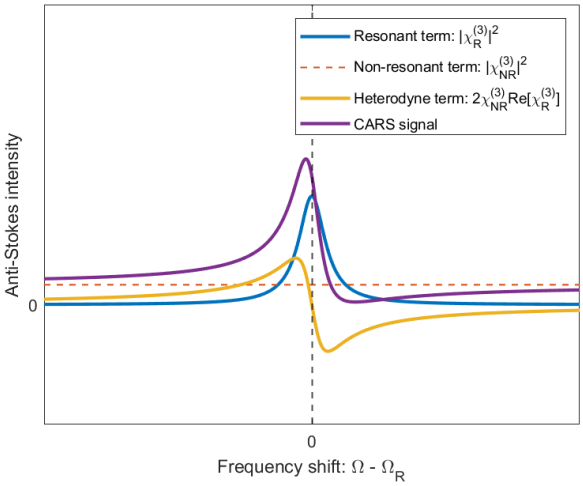

Figure 1: Anti-Stokes signal in the spectral domain: the contributions from the resonant, non-resonant and heterodyne terms are highlighted.

The NRB modifies the resonant signal redshifting the maximum of the peaks and consequently distorting them. Since only the resonant term is carrying information regarding the vibrational modes, and therefore is the only meaningful part for spectroscopic applications, it is generally desired to remove the NRB from the CARS signal. In order to remove it, phase retrieval methods can be used. In particular, Kramers-Kronig (KK) relations allow the extraction of the imaginary part of the $\chi_R^{(3)}$, which contains the vibrational information [5].
In the framework of B-CARS, two different mechanism can be distinguished depending on the order of interactions with pump and Stokes pulses: two and three-color CARS, which are schematically shown in fig. 2.

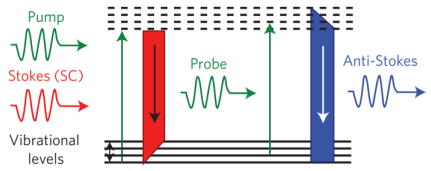

(a) Two-color CARS.

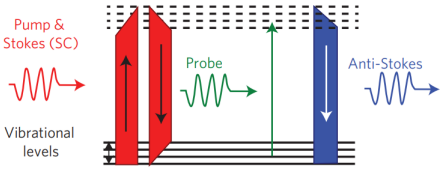

(b) Three-color CARS.

Figure 2: Jablonsky diagram of (a) Two-color and (b) Three-color CARS. Adapted from [2].

In two-color CARS, the first interaction between light and matter is with a pump photon, promoting the molecule to a virtual level, subsequently, the molecule, stimulated by the Stokes photon, decays reaching a vibrationally excited level. In the B-CARS picture, due to the broad spectrum of the Stokes pulse, many levels can be reached. Then, another pump photon acts as a probe, exciting the molecule to other virtual levels. Finally, the molecule decays emitting an anti-Stokes photon, giving rise to the CARS signal. On the other hand, in three-color CARS, the first interaction is with a Stokes photon (which acts as a pump), which excites the molecule to a virtual level. Then, due to a second interaction with the Stokes pulse, it decays to a vibrational level. Therefore, it is possible to observe this process only if the Stokes pulse is compressed, thus all the colors reach the sample simultaneously. Indeed, to successfully excite a mode of vibration, the time duration of the pulses should be lower or comparable to the oscillation period associated to that mode. Subsequently, as in two-color CARS, a pump photon acts as a probe; the molecule reaches a virtual level and then decays emitting an anti-Stokes photon. In this work, we demonstrate that in our B-CARS system both the mechanisms are exploited for obtaining wide spectra spanning from 400 to 3100 cm^{-1}.

3. Experiments and results

3.1. Experimental set-up

The experimental set-up is based on a laser source (Monaco 1035, Coherent): a fiber-based Ytterbium pulsed laser system with a central wavelength at $\lambda_0 = 1035$ nm and a spectral bandwidth of 10 nm. A scheme of such set-up is depicted in fig. 3.

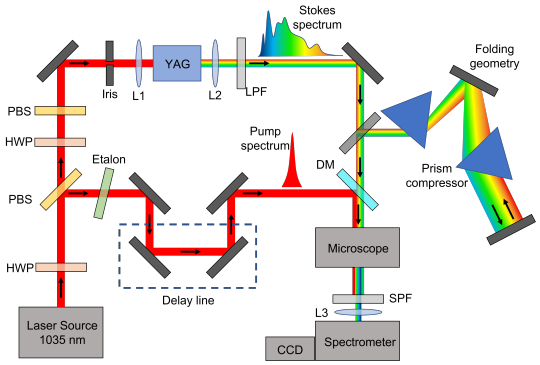

Figure 3: Scheme of the experimental set-up.

For the experiments performed, a total output optical power of ≈ 5 W, a pulse duration of ≈ 270 fs and a repetition rate of 2 MHz have been chosen. The combination of a half-wave plate (HWP) and a polarizing beam splitter (PBS) allows us to divide the initial beam into two replicas. The first replica passes through an etalon, which shrinks the bandwidth, generating narrowband pump pulses. The other replica is focused in a 10-mm-thick YAG crystal initiating SC generation, broadening the spectrum up to 1600 nm, giving rise to the broadband Stokes pulse. Afterwards, a long-pass filter (LPF) selects the red shifted lobe of the SC (1050 or 1200-1600 nm). Then, to compensate for the group delay dispersion introduced by the optical elements, in particular by the microscope objectives, the Stokes pulse propagates through a prism compressor. Depending on the compression of the Stokes pulse and on the LPF used, we generate two or three-color CARS signal. The spatiotemporal superposition of the two beams is realized using a dichroic mirror and a manual delay line mounted on the pump beam path. Then, the pulses interact with the sample in a home-build confocal microscope giving rise to the CARS signal which is focused on a spectrometer (Acton SP2150, Princeton Instrument), with a 600 gr/mm grat-

ing, which separates the different wavelengths. Then, the various frequencies reach a high-speed back-illuminated CCD Camera (BLAZE, Teledyne Princeton Instruments), characterized by an image area of 100×1340 pixels. The configuration described is used to perform high speed imaging in a raster scanning fashion.

3.2. Experimental results

To assess the performance of our B-CARS system, we performed spectroscopy measurement on some solvents (DMSO, Toluene, Ethanol, Methanol, Isopropanol and Acetone), reaching high-speed acquisition (<1 ms/spectrum), and subcellular acids (Palmitoleic, Arachidonic, Linoleic, Oleic and Docosahexonic acids). Once the B-CARS spectra are detected, KK relations are exploited to extract the vibrational information. Afterwards, they are compared to SR spectra, obtaining an excellent agreement. An example of such measurements is shown in fig. 4.

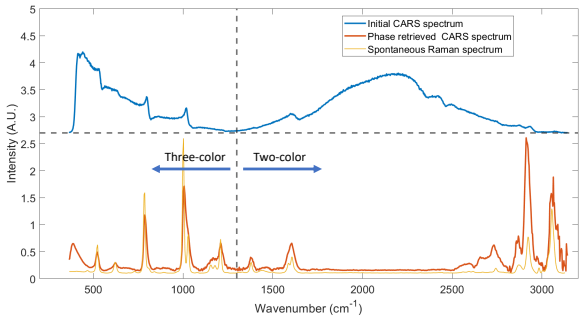

Figure 4: Two and three-color B-CARS spectra before and after NRB removal and spontaneous spectrum of Toluene. Integration time: 1.2 ms.

We also performed imaging on test samples, made of PS and PMMA beads immersed in DMSO, in order to test the ability of our set-up to distinguish different chemical species. The raw data consist of hyperspectral cubes, which are denoised through SVD decomposition. Afterwards, the NRB is removed through KK and MCR-ALS algorithm is applied, allowing us to retrieve the spectra of the different species (see fig. 5a) and their concentration map, which is used to generate false color images (see fig. 5b) highlighting the various chemical constituents.

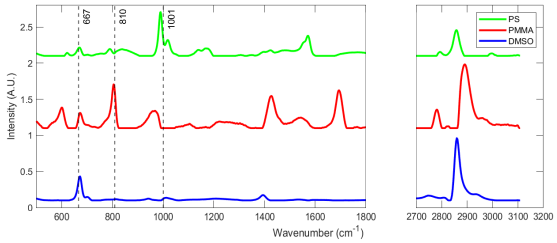

(a) Spectra of the different chemical species.

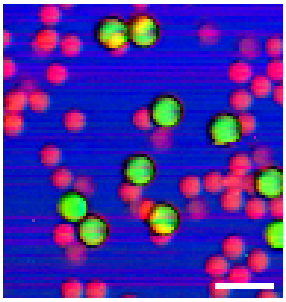

(b) False color image.

Figure 5: (a) Spectra of the different chemical species and (b) False-colours image of test sample. Blue for DMSO, red for PMMA beads, green for PS beads. Scale bar: 20 μm. Pixel dwell time: 10 ms, Spectra per second: 100.

Finally, we applied the same procedure to biological samples.

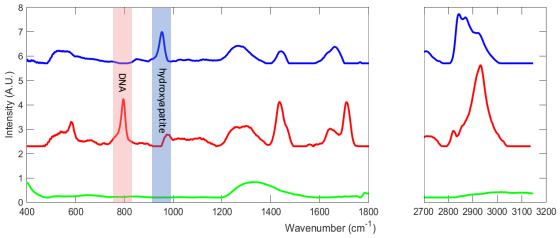

(a) Spectra of the different chemical species.

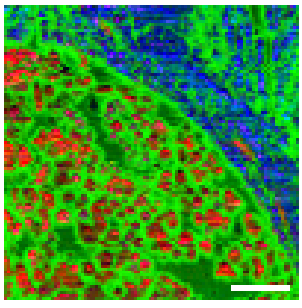

(b) False color image.

Figure 6: (a) Spectra of the different chemical species and (b) False-colours image of a murine vertebra. Blue: bone, red: marrow, green: background. Scale bar: 20 μm. Pixel dwell time: 10 ms, Spectra per second: 100.

In fig. 6, we show the results obtained analyzing a murine vertebra. Analyzing the fingerprint region of the first spectrum (in blue), we can observe an intense band between 940-980 cm^{-1}, which is associated to phosphate bonds in hydroxyapatite, while the second spectrum (in red) is characterised by the presence of a band at ≈ 790 cm^{-1}, typically assigned to DNA, mainly found in cells. These features allow us to assign the blue spectrum to bone and the red one to marrow.

4. Conclusions

In this work, we showed how our home-build experimental set-up allows us to successfully execute high-speed spectroscopy and imaging acquiring B-CARS spectra via the two and three color mechanisms, covering the whole Raman active region. We successfully performed post-processing analysis of the hyperspectral data exploiting SVD, KK and MCR-ALS algorithms. We tested the ability to distinguish different species in heterogeneous samples, which paves the way to future bio-medical applications, such as cancer diagnosis.

References

[1] Dario Polli, Vikas Kumar, Carlo M. Valensise, Marco Marangoni, and Giulio Cerullo. Broadband coherent raman scattering microscopy. *Laser & Photonics Reviews*, 12(9):1800020, 2018. doi: https://doi.org/10.1002/lpor.201800020. URL `https://onlinelibrary.wiley.com/doi/abs/10.1002/lpor.201800020`.

[2] Charles H. Camp Jr, Young Jong Lee, John M. Heddleston, Christopher M. Hartshorn, Angela R. Hight Walker, Jeremy N. Rich, Justin D. Lathia, and Marcus T. Cicerone. High-speed coherent raman fingerprint imaging of biological tissues. *Nature Photonics*, 8(8):627–634, Aug 2014. ISSN 1749-4893. doi: 10.1038/nphoton.2014.145. URL `https://doi.org/10.1038/nphoton.2014.145`.

[3] Hideaki Kano and Hiro-o Hamaguchi. Ultrabroadband (>2500cm^{-1}) multiplex coherent anti-stokes raman scattering microspectroscopy using a supercontinuum generated from a photonic crystal fiber. *Applied Physics Letters*, 86(12):121113, 2005. doi: 10.1063/1.1883714. URL `https://doi.org/10.1063/1.1883714`.

[4] Federico Vernuccio, Arianna Bresci, Benedetta Talone, Alejandro de la Cadena, Chiara Ceconello, Stefano Mantero, Cristina Sobacchi, Renzo Vanna, Giulio Cerullo, and Dario Polli. Fingerprint multiplex cars at high speed based on supercontinuum generation in bulk media and deep learning spectral denoising. *Opt. Express*, 30(17):30135–30148, Aug 2022. doi: 10.1364/OE.463032. URL `http://opg.optica.org/oe/abstract.cfm?URI=oe-30-17-30135`.

[5] Charles H. Camp, Young Jong Lee, and Marcus T. Cicerone. Quantitative, comparable coherent anti-stokes raman scattering (CARS) spectroscopy: correcting errors in phase retrieval. *Journal of Raman Spectroscopy*, 47(4):408–415, October 2015. doi: 10.1002/jrs.4824. URL `https://doi.org/10.1002/jrs.4824`.